Methane Emission from a Tropical Wetland in Ka‘au Crater, O‘ahu, Hawai‘i[1]

Maxime Grand[2,4] *and Eric Gaidos*[3]

Abstract: Natural tropical wetlands constitute an important but still poorly studied source of atmospheric methane, a powerful greenhouse gas. We measured net methane emission, soil profiles of methane generation and oxidation, and related environmental parameters in a tropical wetland occupying the Ka‘au extinct volcanic crater on the Hawaiian island of O‘ahu. The wetland has a fluctuating water table with dynamics that can be reproduced using precipitation data and a simple model. Median net methane flux was 117 mg m^{-2} day^{-1} and is consistent with measurements at other tropical sites. Net methane flux in the *Commelina diffusa*–dominated vegetation pattern (honohono) was significantly higher than that of the invasive *Psidium cattleianum*–dominated pattern (strawberry guava). Net methane emission in the honohono vegetation pattern was also significantly higher during the "wet" season compared with the "dry" season, although we did not find a clear correlation between net methane emission, water table level, or precipitation. We show that the measured fluxes are consistent with the integrated potential methane generation over the uppermost 30 cm of soil and consumption of ~50% of that methane in the soil. Absence of a correlation between net methane emission and water table level may be due to suppression of the activity of strictly anaerobic methanogens by dynamic redox conditions in the upper layers of soil and varying rates of methane oxidation by facultive methanotrophs.

Atmospheric methane (CH_4) is a powerful greenhouse gas responsible for 20% of the anthropogenic change in direct radiative forcing (Intergovernmental Panel on Climate Change 2001). Its concentration has more than doubled since the preindustrial era, although its annual increase of ~1% has slowed in the last two decades (Dlugokencky et al. 1998). Wetlands constitute an important natural source of atmospheric CH_4, and boreal wetlands have been intensely studied in this context (Chapin et al. 2000, Wuebbles and Hayhoe 2002). Natural tropical wetlands, however, are more poorly studied, despite their relatively larger contribution to atmospheric methane (Bartlett and Harriss 1993, Milich 1999, Marani and Alvala 2007). Much of the work at low latitudes has been limited to the Amazonian floodplain and Florida Everglades (e.g., Bartlett et al. 1989, Devol et al. 1990) and restricted to area-averaged estimates of methane flux.

In wetlands, methane is the end product of the anaerobic decomposition of organic matter in flooded soils rendered anoxic by the low diffusivity of oxygen through pore water. Net methane emission is the difference between production by methanogenic archaea in water-logged anoxic zones, and aerobic methane oxidation by methanotrophic bacteria in any aerated zones of soil and in vascular plant tissue. Numerous studies have shown

[1] This research was partly supported by an award from the University of Hawai‘i Research Training Revolving Fund to E.G. and a Global Environmental Sciences Fellowship for Senior Thesis Research to M.G. Manuscript accepted 10 February 2009.

[2] Department of Oceanography, University of Hawai‘i at Mānoa, Honolulu, Hawai‘i 96822.

[3] Department of Geology and Geophysics, University of Hawai‘i at Mānoa, Honolulu, Hawai‘i 96822.

[4] Corresponding author: (e-mail: maxime@hawaii.edu).

Pacific Science (2010), vol. 64, no. 1:57–72
doi: 10.2984/64.1.057

that CH_4 flux depends sensitively on whether the water table is above or below the soil surface (Funk et al. 1994, Roslev and King 1996, Rask et al. 2002) rather than the actual depth of standing water (Harriss et al. 1988, Bartlett et al. 1989, Bartlett et al. 1990, Devol et al. 1990, Moore et al. 1994, Kettunen et al. 2000, Ding et al. 2004). Thus the extent, rather than degree, of flooding may control total methane emission. Climate models predict that future global warming will alter patterns of precipitation, particularly in the continental tropics (Wetherald and Manabe 2002, Watterson and Dix 2003), affecting the surface extent and thus total methane emission of wetlands there (Moore 2002).

Vascular plants provide a conduit both for CH_4 to the atmosphere and for O_2 to the soil, the latter often supporting methanotrophic bacteria in the plant rhizosphere. As such, differences in vegetation may affect net methane emission. For example, C3 plants have a higher stomatal conductance for the same rate of photosynthesis as C4 plants and thus would conduct methane to the atmosphere at a higher rate. Conversely, many wetland plants conduct more oxygen to their root systems; this increased conductance increases the potential for in situ methane oxidation (Gerard and Chanton 1993, Le Mer and Roger 2001).

We measured net methane emission, potential methane production, and methane oxidation in a tropical wetland occupying the extinct Ka‘au volcanic crater on the Hawaiian island of O‘ahu (21° 20′ 00″ N, 157° 46′ 30″ W) during a 1-yr study period starting in August 2003. In this wetland, the water table is always close to, or slightly above, the surface of the soil and is maintained by high annual precipitation rather than poor drainage, thus giving the crater a dynamic hydrology. Our objectives were to: (1) estimate the methane flux from this wetland; (2) quantitatively assess differences in methane emission with precipitation and vegetation pattern; and (3) interpret these variations in terms of the distribution of potential methane production and methane oxidation with depth in the soil and the time-response of these quantities to changing environmental conditions.

Study Site

Ka‘au Crater is a 450 m diameter explosion crater (~0.16 km^2) that formed during the postshield-building Honolulu Volcanic Series of eruptions on O‘ahu. The crater is located immediately southwest of the crest of the Ko‘olau Range (21° 20′ N), and its floor is at an elevation of 463 m. The underlying units of the Ko‘olau shield volcano have a high hydraulic conductivity (~20 m hr^{-1}) (Oki et al. 1999); however the crater itself was initially occupied by a lava lake (Macdonald et al. 1983) that created a relatively impermeable floor. Surface drainage occurs through a single breach in the crater wall. The estimated flow rate of the stream approximately equals the average input of precipitation into the crater (~30 liters sec^{-1} [E.G., unpubl. data]), although subsurface drainage is possible. Today, peat soil has accumulated in the crater to a depth exceeding 3.6 m (Hotchkiss and Juvik 1999). Ka‘au Crater experiences a subtropical climate with a weak seasonality and receives high annual precipitation (~415 cm) that is predominantly orographically controlled.

Kennedy (1975) described five major vegetation patterns in the crater: The largest is dominated by the native sedge *Cladium mariscus* (identified as *Cladium leptostachym* [‘uki] by Kennedy [1975] and *Cladium jamaicense* by Elliot and Hall [1977]). A second major type is a floristically diverse open scrub that includes dwarfed *Metrosideros polymorpha* (‘ōhi‘a). A third type consists almost entirely of *Cordyline terminalis* (ti) with minor incursions of *Commelina diffusa* (honohono) and the bulrush *Shoenoplectus lacustris* (hereafter referred to as the honohono meadow). The final pattern is a dense forest of the invasive *Psidium cattleianum* (strawberry guava) that occupies the crater floor in the vicinity of the outlet stream and the inner slopes of the crater wall. Although the crater lies within the Honolulu Watershed Reserve it has experienced anthropogenic disturbance, including the possible construction of a Polynesian fish pond (Elliot and Hall 1977), an attempt to construct a reservoir by damming the outlet stream (Elliot and Hall 1977), and the introduction of feral pigs.

MATERIALS AND METHODS

Environmental Parameters

Precipitation in Ka'au Crater was monitored with a tipping bucket rain gauge (RG2-M) and data logger (HOBO Micro Station, Onset Computer Corp., Bourne, Massachusetts) placed at 21° 19.68′ N, 157° 46.30′ W. The rainfall record of a NOAA cooperative rain gauge located 2 km distant and 160 m lower (Palolo Valley, no. 718, 21° 18.73′ N, 157° 46.83′ W) was obtained from the NOAA National Climatic Data Center server (http://www.ncdc.noaa.gov). Water-table level in Ka'au Crater was measured from October to November 2003 and February to July 2004 using a sensor (miniTROLL, In-Situ, Fort Collins, Colorado). The sensor was placed in a pipe that was drilled at 5 cm intervals along its length and inserted 50 cm into the soil of the honohono vegetation type throughout the study period. All water-table level data presented are daily averages in centimeters. One-meter air temperature was continuously recorded at 5-min intervals from August to November 2003 using a humidity/temperature data logger (SP-2000, Veriteq Instruments, Richmond, British Columbia, Canada).

Net Methane Emission

We made 82 measurements of net methane emission by the closed flux chamber technique (Schütz and Seiler 1989) using two identical chambers during a 1-yr study period (30 August 2003 to 12 August 2004). Each chamber consisted of a partially translucent polyethylene cylindrical container 106 cm high and 63 cm in diameter, with walls 3 mm thick. Large chambers permit the inclusion of vascular plants that are an important conduit for methane from the soil in many wetlands (Le Mer and Roger 2001). Each chamber was sealed using foam gaskets and clamps to a galvanized aluminum collar that was previously inserted ~10 cm into the soil, establishing a gas-tight seal. A battery-powered fan maintained circulation within each chamber. Thirty-milliliter gas samples were withdrawn at 30-min intervals through a butyl rubber stopper in the top of the chambers. These were injected into previously evacuated 10 ml serum bottles, establishing a positive pressure. To verify the repeatability of our chamber-sampling technique, some gas samples were stored by displacing water from vials. After 90 to 120 min incubation, each chamber was removed and flushed with air between successive measurements. The aluminum collar was left in place if the next measurement was at the same location.

Gas samples were taken to the laboratory and analyzed within 24 hr of collection using a gas chromatograph (GC) (310C, SRI Instruments, Torrance, California) equipped with a flame ionization detector and a T 80/100 column (Hayesep, Alltech Assoc., Deerfield, Illinois). The column was maintained at 35°C, and 30 ml min^{-1} of grade-6 helium (Gaspro, Honolulu, Hawai'i) was used as the carrier gas. The GC was calibrated initially and every 10 analysis runs with a 100 ppm CH_4 standard (Matheson Tri Gas, Montgomeryville, Pennsylvania). Atmospheric samples (~1.85 ppm) were also run. Methane fluxes were calculated from the difference between the initial and final concentrations in the chambers, adjusted for their volumes, surface coverage, and incubation time. All fluxes are reported in units of milligrams of methane m^{-2} day^{-1}. Chamber gas samples collected at 30, 60, and 90 min were used to determine the linearity of methane accumulation within each chamber to identify any decrease in the rate of methane accumulation. The accuracy of individual CH_4 measurements was determined by withdrawing four replicate samples at the final time point of several experiments. Many measurements were also immediately repeated after flushing the chamber. To investigate the effect of water-table level on net methane emission, one chamber was maintained at a fixed location in the vicinity of the water-level sensor within the honohono meadow vegetation type. In the meantime, the other chamber was deployed simultaneously in different locations to evaluate the effect of vegetation on methane flux. During an 8-week period, the chambers were positioned next to each

other to determine the repeatability of the measurements and possible small-scale spatial variability in methane emission. This allowed assessing the statistical significance of any difference in flux between two different vegetation types.

Methane Generation Potential and Methane Oxidation

Six soil cores 18–32 cm deep were collected next to the chamber measurement sites with an AMS soil corer fitted with a plastic pipe (length, 46 cm; diameter, 7 cm) and taken to the laboratory within 3 hr. These were sectioned at 4 cm vertical intervals and then subdivided longitudinally into four subsamples. Methane generation potential was measured by incubating duplicate subsamples from each 4 cm section in 160 ml serum bottles with 25 ml of sterile deionized water and a magnetic stir bar to turn the soil into slurries. Each bottle was sealed using butyl rubber stoppers and aluminum crimp seals and their headspace flushed with nitrogen gas for ~5 min while the slurry was stirred. Headspace gas samples were extracted immediately after stirring and again after 24 hr of incubation at 22°C. To verify that any headspace methane in these incubations was the product of biological activity (and not the release of previously produced methane), another bottled soil sample was heated to 121°C for 1 hr using a steam sterilizer (SM510, Yamato Scientific America, Orangeburg, New York) and incubated as the others. Headspace volumes were measured and the soil was dried for 48 hr at 60°C and weighed. (We found that no further water loss occurred after 24 hr of drying.) Methane generation potential was calculated as the difference between the final and initial methane headspace concentrations adjusted for the bottles headspace volumes and normalized by the dry weight of soil incubated. All data are presented in units of milligrams (g dry soil)$^{-1}$ day^{-1}.

Methane oxidation was measured by incubating the remaining subsamples in duplicate 160 ml serum bottles that were sealed with ambient headspace to which 25 µl of natural gas were added to produce an initial methane concentration between 50 and 200 ppm. Headspace samples were withdrawn and analyzed initially and after 6, 12, and 24 hr of incubation at 22°C while the samples were continuously agitated at 120 rpm to prevent the onset of anoxia in the soil. Negative controls were prepared by autoclaving at 121°C and incubating them in the same manner. At the end of the experiments, the bottle headspace volumes were measured and the slurries dried and weighed as previously described. Methane oxidation rate constants were calculated assuming first-order kinetics and data were fitted to an exponential function. All fits had a coefficient of determination $R^2 > 0.95$ and all but two fits had $R^2 > 0.99$. Rate constants were normalized by the dry weight of soil and are reported as hr^{-1} (g dry soil)$^{-1}$.

Plant-Associated Methane Oxidation

Our protocol is derived from that of Heilman and Carlton (2001). Briefly, root and stem samples (the latter from the soil level and several centimeters above) of the species *Cladium jamaicense* and *Shoenoplectus lacustris* were collected and immediately transported to the laboratory. All root and basal stem samples were rinsed to remove soil particles and ensure that any methane oxidation activity occurring was from methanotrophs located within or attached to the plant tissue. Each sample was then placed in 25 ml serum bottles with 2–3 ml water, and 25 µl methane was added to the headspace to achieve an initial concentration of 50–200 ppm. Changes in the methane concentrations were monitored after 0, 1, 2, 3, and 24 hr of incubation as described earlier.

Soil Analyses

Soil pH profiles were obtained in the hono-hono, ʻōhiʻa, and strawberry guava vegetation types using a previously described protocol (Van Lierop 1990) where 2.5 g of oven-dried and sieved soil and 5 ml of sterile, deionized H_2O were added to 10 ml Falcon tubes. Each tube was vortexed for ~1 min, and solids within the solution were allowed to settle for

1 hr. The pH of the supernatant was measured (Accumet AB 15 Plus meter, Fisher Scientific, Pittsburgh, Pennsylvania). pH was also measured in several standing bodies of water in the wetland. Soil samples were analyzed at the University of Hawai'i College of Tropical Agriculture and Human Resources Agricultural Diagnostic Service Center for nitrogen, organic carbon, and sulfur content (three to nine replicate samples for nitrogen and organic carbon).

Statistical Analyses and Water-Table Level Model

Differences in methane fluxes between different vegetation types and between wet and dry season were tested using the Student *t*-test assuming unequal variances when significant heteroskedasticity was detected. All statistical analyses were performed using Microsoft Excel 2004. We report median net methane emissions in addition to average emissions because median values are less subject to outliers and thus may reveal smaller effects or trends. Water-table level in Ka'au Crater was modeled using IDL software (ITT Corporation).

RESULTS

We measured daily rainfall in Ka'au Crater during 178 days in 2003 (9 February–25 October). Measurements were terminated by the failure of the rain gauge's data logger. The measurements show a linear correlation with records at the Palolo Valley station ($R^2 = 0.95$), with the Ka'au Crater site receiving 25% more rainfall (data not shown). Missing precipitation data in the 1-yr study interval was estimated using the Palolo Valley station and our linear regression results. The average precipitation at the Palolo Valley station over the past 55 yr is 332 cm, and the daily average rainfall is 9 mm (Figure 1). We therefore estimate that Ka'au Crater received 415 cm of annual precipitation during the same period. The Palolo Valley historical data indicate a weak seasonality of about 30% in precipitation, with the wettest season extending from 31 October to 20 May (Figure 1). The historical record also shows a rainfall minimum in February of short extent (~20 days [Figure 1]) that we included in the "wet" season in the following discussion. We measured temperature on 105 days during the "dry" season and 108 days during the "wet" season. The average air temperature in the crater is 21.5°C, the standard deviation in daily-averaged temperature was 1.9°C, and the wet-dry seasonal difference was 2.7°C.

Water-table level was measured from 29 September to 2 November 2003 and from 12 February to 13 June 2004 (Figure 1). The level is characterized by fluctuations of up to 20 cm on timescales of days. It reached the soil surface, but surface water was always of negligible depth, probably because of efficient drainage from the wetland surface. The water-table level fluctuations were highly correlated with precipitation events. We found that the water-table level on the nth day h_n can be modeled by the recursive relationship

$$h_n = h_{n-1}\left(1 - \frac{1}{\tau}\right) + Ap_{n-1},$$

where τ is a drainage time constant in days, p_n is the precipitation on the nth day, and A is a factor that accounts for a watershed larger than the crater rim. Water level is constrained to be

$$-H \le h \le 0,$$

where H is the water-table depth at which drainage out of the wetland becomes negligible. In the absence of precipitation, the water-table level decays exponentially on a timescale τ toward this level. We found that the parameter values $\tau = 8.3$ days, $A = 1.75$, and $H = 18$ cm reproduce two major water-table level excursions in our data, but that no single set of parameters can reproduce the detail of all excursions (data not shown), possibly because of sinking or tilting of the water-level sensor over time.

The average soil pH was 4.9 ($n = 19$) and did not vary significantly with vegetation pattern or depth ($P = 0.21$). This is close to the average pH (5.5) of open bodies of water in the wetland. Average organic carbon, nitrogen, and sulfur contents (by weight) were 37% ($n = 16$), 2.4% ($n = 16$), and 80 ppm

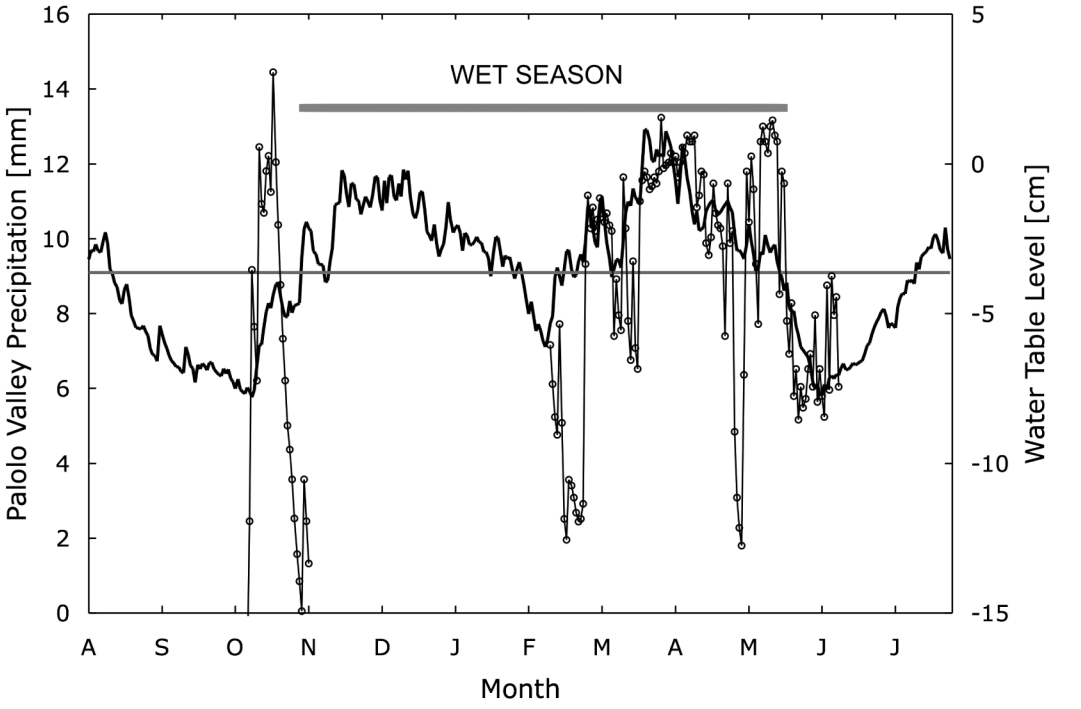

FIGURE 1. Daily precipitation in Palolo Valley averaged over the past 55 yr. Data from NOAA National Climatic Data Center Palolo Valley Station no. 718. Black line shows daily average precipitation (9 mm day^{-1}), which we used to define the extent of the wet season (thick gray line). Connected open circles are water-table level in Ka'au Crater measured during two intervals in 2003–2004.

($n = 3$), respectively (Table 1). The difference in the mean nitrogen contents of the soil in the sedge (2.6%) and strawberry guava (1.9%) vegetation patterns was significant ($P = 0.03$).

Eighty-two measurements of net methane emission over the 1-yr study period are tabulated in Appendix 1. Dense vegetation limited the spatial distribution of chamber measurements to the honohono, strawberry guava, 'ōhi'a and native sedge vegetation patterns near the crater outlet only. The repeatability of our GC measurements was 0.25 ppm at atmospheric (1.85 ppm) CH_4 concentrations. The standard deviation among replicate chamber samples was 0.65 ppm ($n = 15$). The standard deviation among replicate samples stored in water-filled serum vials was slightly smaller (0.4 ppm), but there was no significant difference in fluxes calculated

TABLE 1

Soil Organic Carbon, Nitrogen, and Sulfur Content

Vegetation Pattern	Organic Carbon [%]	Total Nitrogen [%]	Sulfur [ppm]
Honohono	35 ± 3 ($n = 3$)	2.8 ± 0.3 ($n = 3$)	81 ($n = 1$)
Strawberry guava	41 ± 5 ($n = 5$)	1.9 ± 0.3 ($n = 5$)	53 ($n = 1$)
Sedge	34 ± 6 ($n = 8$)	2.6 ± 0.7 ($n = 8$)	110 ($n = 1$)

TABLE 2

Net Methane Emission Statistics (Units are mg CH_4 m^{-2} day^{-1})

Sample	*n*	Median Flux	Average Flux	Std. Dev	Std. Error
All valid	68	117	126	84	10
Honohono	53	145	151	72	10
ʻŌhiʻa	4	43	82	107	53
Strawberry guava	8	15	22	28	10
Sedge	3	17	17	8	5
Honohono (dry season)	15	77	93	56	14
Honohono (wet season)	38	165	174	65	11

from samples stored in evacuated vials or water-filled vials. For a typical 90-min experiment our minimum detectable (3σ) methane flux was 6.5 mg CH_4 m^{-2} day^{-1}. Our detection threshold is high compared with many other studies because of our on-column injection system and the large chambers used for the inclusion of plants. The median percentage difference between fluxes in 30 pairs of duplicate experiments in which both chambers remained in place was 7.0%. Measurements used to determine the accuracy and variability of our measurements are denoted by a "V" in Appendix 1.

Steady accumulation of methane within a chamber should produce a linear trend in CH_4 concentration. A reduced chi-squared (χ^2_υ) was calculated for a linear fit to each experiment assuming 0.65 ppm experimental error (Appendix 1). In some of our experiments the CH_4 concentration deviated significantly from linearity, often reaching an asymptotic value, and it was necessary to eliminate time points or entire experiments (Appendix 1).

The median of all valid flux measurements is 117 mg CH_4 m^{-2} day^{-1} ($n = 68$), and the average is 126 ± 10 mg CH_4 m^{-2} day^{-1} (Table 2). Figure 2 plots the 51 measurements (two nondetections not shown) in the honohono vegetation pattern and 1-month averaged precipitation in Kaʻau Crater estimated from the Palolo Valley data. We show 1-month averaged precipitation rather than a higher resolution (daily or weekly) to reveal seasonal trends. The comparison reveals that, during our study period, the largest methane emissions in the honohono pattern occurred during the wet season and that there seems to be a delay (>30 days) between the highest rainfall events and the highest net methane fluxes recorded. The median values in the honohono meadow only during the "dry" and "wet" seasons were 77 mg CH_4 m^{-2} day^{-1} ($n = 15$) and 165 mg CH_4 m^{-2} day^{-1} ($n = 38$), respectively (Figure 2, data indicated with an "S" in Appendix 1). The difference in the mean values for the honohono meadow during the "dry" and "wet" seasons (93 and 174 mg CH_4 m^{-2} day^{-1}, respectively [Table 2]) is significant ($t = 7.2$, $\mathrm{df} = 47$, $P = 2.4 \times 10^{-4}$).

The median values of fluxes measured in the honohono, ʻōhiʻa, native sedge, and strawberry guava vegetation patterns are also reported in Table 2. The limited sample sizes in the sedge and ʻōhiʻa vegetation patterns prevent us from drawing statistically meaningful conclusions, but measurements in the honohono (mean = 151 mg CH_4 m^{-2} day^{-1}, $n = 53$) were significantly higher than those in the strawberry guava (mean = 22 mg CH_4 m^{-2} day^{-1}, $n = 8$; $t = 7.5$, $\mathrm{df} = 24$, $P = 3.7 \times 10^{-8}$).

Profiles of methane-generation potential are shown in Figure 3 (the autoclaved negative control produced no detectable methane). In all three honohono profiles and one of the guava profiles there is a peak in the methane-generation potential at a depth of 10 cm. However, in the ʻōhiʻa profile the maximum in methane-generation potential is at the surface. We found an exceptionally high rate of methane generation in the core

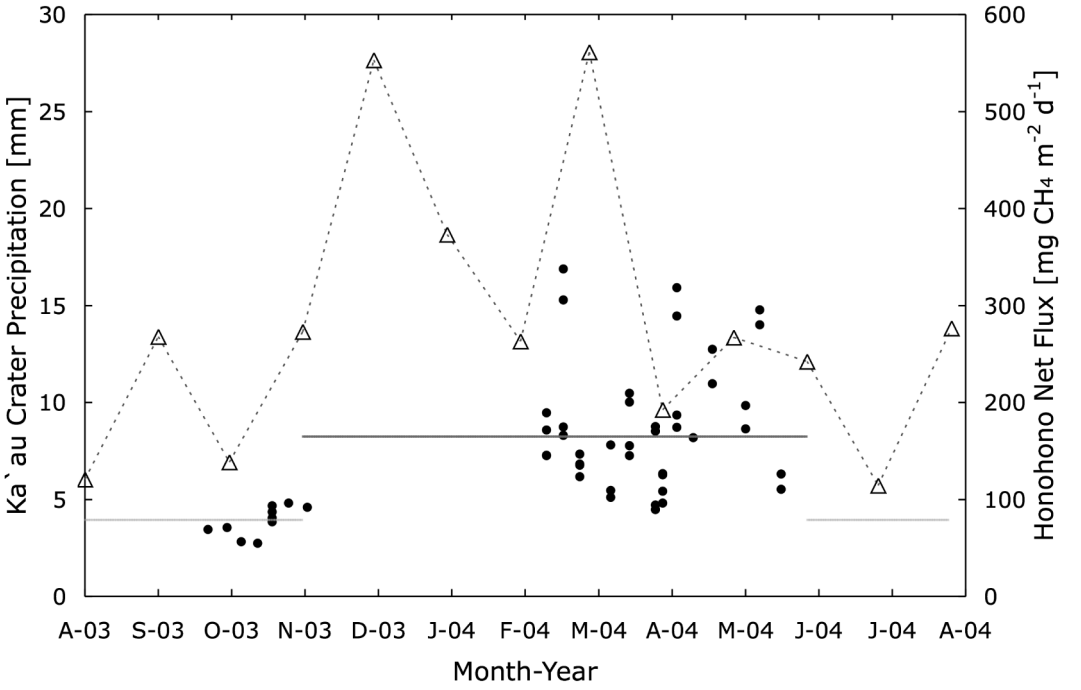

FIGURE 2. Net methane flux in the honohono vegetation pattern (filled circles) and 1-month average precipitation in Ka'au Crater wetland (open triangles) over the 1-yr study period. Ka'au Crater precipitation data derived from correlation with Palolo Valley Station no. 718. Nondetections not shown. Median values during the dry (gray line: 77 mg CH_4 m^{-2} day^{-1}) and wet seasons (dark line: 165 mg CH_4 m^{-2} day^{-1}) are shown.

obtained from the honohono vegetation pattern on 28 March 2004.

Profiles of methane oxidation in intact core samples are shown in Figure 4. Compared with methane-generation potential, these profiles do not exhibit order-of-magnitude variations with depth in different vegetation patterns and sampling times. In all cores but the strawberry guava of 5 May 2004, in situ oxidation rate constants show a pronounced peak between 14 and 18 cm depth. We also carried out 86 experiments to measure methane oxidation in roots and stem material of the species *Cladium jamaicense* and *Shoenoplectus lacustris*. In only six experiments was there a significant decrease in methane concentration, all associated with the bulrush *Shoenoplectus lacustris*. However, 57 bulrush samples did not exhibit this trend, and no clear pattern of plant-associated methane oxidation emerged from these experiments.

DISCUSSION

The precipitation and water-table level records analyzed here show that the Ka'au Crater has a dynamic water table, which fluctuates with an amplitude of up to 20 cm on a timescale of about 8 days. Using our model of the water-table level and the rainfall record at nearby Palolo Valley, we estimate that the wetland was inundated during 45% of the 1-yr study period beginning 15 August 2003. Despite the presence of five different vegetation groups, the wetland appears remarkably uniform in terms of soil chemistry (Table 1).

Chamber methane-accumulation experiments are subject to several systematic errors, often manifest by nonlinearity of chamber CH_4 concentration versus time. Such behavior can be identified using a criterion such as R^2 (Khalil et al. 1998) or reduced chi-squared (χ^2_υ). Linear fits to several of our experiments

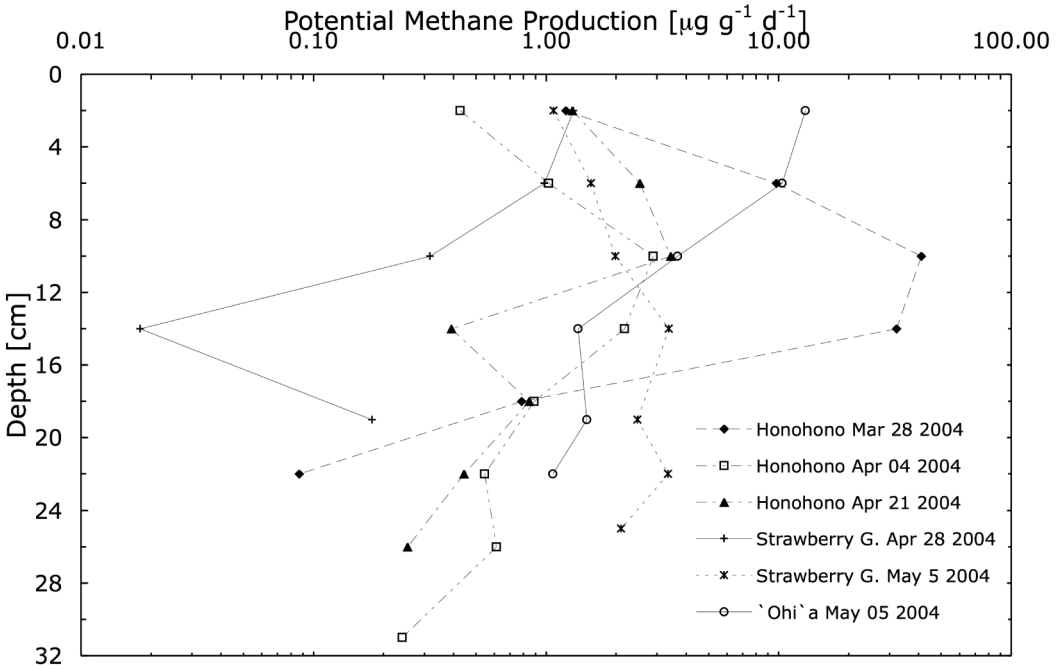

FIGURE 3. Profiles of methane-generation potential versus depth in soil cores from the honohono, strawberry guava, and ʻōhiʻa vegetation patterns.

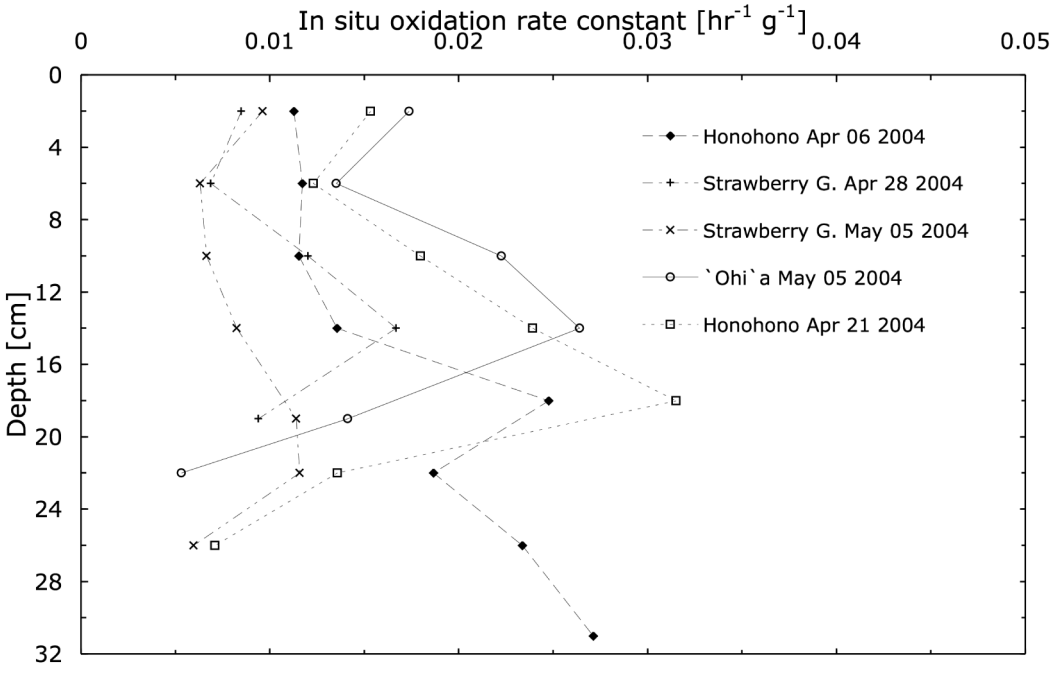

FIGURE 4. Profiles of intact methane oxidation rate in soil cores from the honohono, strawberry guava, and ʻōhiʻa vegetation patterns.

have $\chi_v^2 > 1$. We compare the distribution with $x = \chi_v^2$ for all linear fits with the expected distribution

$$p(x)\,dx = Cx^{-(v-2)/2}e^{-xv/2},$$

where v, the number of degrees of freedom of the fit, is equal to $n - p$, where n is the number of measurements and p is the number of parameters (two). In the majority of our cases (Appendix 1), $n = 4$ and the distribution reduces to $p(x) = exp(-x)$. In that case, the cumulative fraction f of measurements with a χ_v^2 less than a particular value should satisfy

$$\chi_v^2 = -\ln(1 - f)$$

The left- and right-hand sides of this equation are plotted in Figure 5 for all experiments with $n = 4$–6. Experiments with reduced $\chi^2 < 0.5$, about 40% of the total, have the predicted distribution with unit slope. This affirms the estimate of measurement error (0.65 ppm) because an incorrect value would produce a distribution with a slope different than unity.

The other 60% of experiments include some with significant departures from the expected linear accumulation of CH_4 in the chamber. These consist chiefly of abrupt rises in CH_4 concentration at the beginning of an experiment and a decreasing slope in CH_4 versus time at the end of the experiment. Replicate samples of chamber gas obtained using two different storage techniques (evacuated and water-filled vials) produced identical fluxes within the measurement errors, demonstrating that our sample acquisition and analysis methods are not responsible for the observed deviations from linearity. Rather, these deviations reflect the actual concentration of CH_4 with time. High initial methane concentrations (up to 70 ppm) were observed. Such abrupt increases over the atmospheric value could result from release of methane from shallow soil pools by distur-

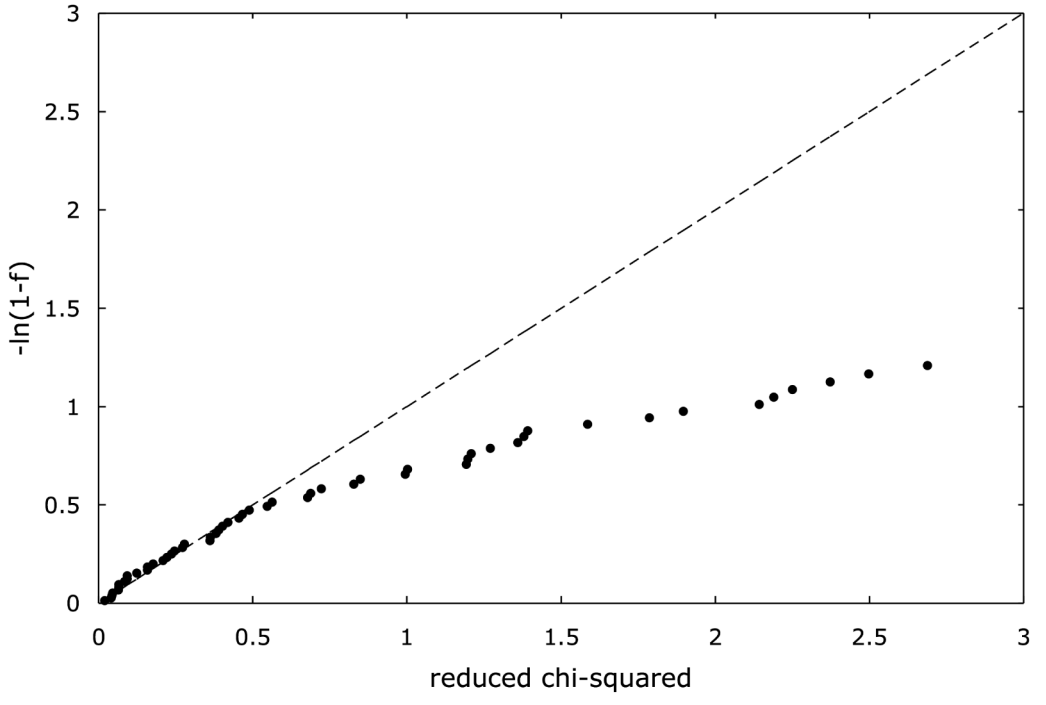

FIGURE 5. Modified cumulative distribution of reduced chi-squared values for all experiments with four to six measurements (points) and the theoretical exponential distribution (dashed line).

bance during setup of the experiment. Such pools can accumulate when the water table reaches the surface and soil aeration effectively ceases.

The lack of a consistent effect in all experiments or with one chamber argues against a chamber leak or thermal stratification in the chamber. A decrease in methane flux from wetland plants because of a reduction in the leaf-to-air concentration gradient has been previously documented (Knapp and Yavitt 1992). However, we consider it unlikely that changes in plant properties (i.e., stomatal conductance due to reduced solar radiation, levels of CO_2, or temperature) during the experiments could be the dominant process responsible for the observed nonlinearity because some of our experiments in the guava and ʻōhiʻa vegetation patterns, which were carried out where ground cover was absent, also exhibited this effect. Rather, as the gradient in methane concentration between the chamber and soil and plant tissues decreases, the flux of CH_4 into the chamber decreases. Khalil et al. (1998) found that this "saturation effect" appears at concentrations of 30 ppm and becomes very large by 60 ppm. We conservatively exclude from further consideration 14 measurements where the *initial* concentration exceeded 30 ppm or reached 30 ppm after 60 min incubation time (indicated in Appendix 1). The latter displayed a decreasing slope in CH_4 versus time after 30 ppm was reached, indicating the incidence of the saturation effect (Khalil et al. 1998). In some cases, outlying time points were eliminated and the net methane flux and χ^2_ν were recalculated accordingly (see notes in Appendix 1).

The median value of our valid Kaʻau Crater net methane-flux measurements (117 mg CH_4 m^{-2} day^{-1}) is comparable with previously published values in natural tropical or subtropical wetlands (Bartlett and Harriss 1993, Marani and Alvala 2007). Although methane production can be temperature-dependent (Segers 1998), the 2.7°C seasonal air temperature difference at Kaʻau Crater is expected to produce little variation (e.g., 20% for a $Q_{10} = 2$ [Van Hulzen et al. 1999]). We computed the cross-correlation between water-table level (measured or inferred from the precipitation record) and net methane emission measured at a fixed site in the honohono vegetation pattern ($n = 19$). We found a maximum correlation between water-table level the previous day and net methane emission in the honohono meadow (Pearson correlation coefficient $r = 0.45$). Monte Carlo calculations with randomly shuffled data sets show that this result is significant ($P = 8.0 \times 10^{-3}$). However, a plot of net methane flux versus previous day's water-table level (Figure 6) shows no obvious correlation and large scatter, particularly when the water level is at the surface. This might be due to a lag ($\geq$30 days) between rainfall events and peaks in net methane flux (Figure 2). The absence of a strong correlation between methane flux and water-table level in permanently flooded wetlands has been previously noted (Harriss et al. 1988, Bartlett et al. 1989, Bartlett et al. 1990, Devol et al. 1990, Moore et al. 1994, Kettunen et al. 2000, Ding et al. 2004).

Our data do not indicate any difference in net methane emission between the honohono and ʻōhiʻa vegetation patterns. However, net methane emission in the honohono was significantly higher than that in the invasive strawberry guava ($P = 3.7 \times 10^{-8}$). We attribute this difference to the lower methane generation potential in the strawberry guava soil at 10 cm depth (Figure 3), where peaks of potential methane production were recorded in all other vegetation patterns studied. Although soil pH and carbon and nitrogen content appeared relatively uniform across vegetation patterns, *Psidium cattleianum* produces heavy leaf and fruit litter containing bioactive compounds (Pino et al. 2004) that suppress the growth of competing plants and perhaps microorganisms such as methanogens (Segers 1998). Alternatively, both methane emission and vegetation could reflect an independent variable such as microtopography. Although the area where the strawberry guava was located was lower than the remaining wetland, its surface was consistently better drained, perhaps because of higher soil permeability and its proximity to the outlet stream.

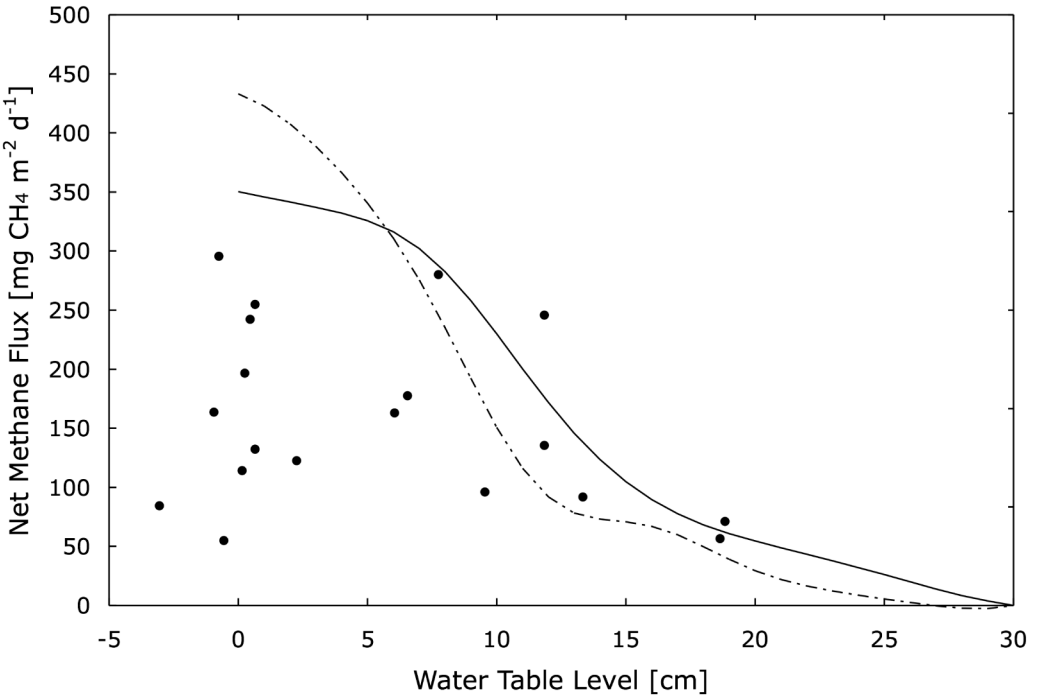

FIGURE 6. Net methane flux versus water-table level in the honohono vegetation pattern. The curves are the integrated methane flux based on the profiles of potential methane production from soil cores in the honohono pattern obtained on 6 April 2004 (solid curve) and 21 April 2004 (dashed curve). The calculations assume that methane is produced only in soil below the water table and ignores methane consumption.

Profiles of methane production and consumption indicate the presence of active methanogens and methanotrophs throughout the uppermost 30 cm of wetland soil (Figures 3 and 4). The increase in methane generation potential with depth in the honohono core probably reflects an increased abundance of strictly anaerobic methanogens. The relative variation in methane oxidation is much smaller, probably the result of a greater tolerance of methane oxidizers for both aerobic and anaerobic conditions (Roslev and King 1996).

Given a profile of potential methane generation and assuming that the oxic-anoxic interface corresponds to the water-table level, the dependence of methane production on water-table level can be estimated and compared with observed trends. In Figure 6, we plot estimated flux versus water-table depth based on the integration of two profiles of methane-generation potential obtained in the honohono meadow in April 2004, along with actual net methane-emission observations. A dry-soil specific gravity of 1.2 is assumed. This calculation ignores any latency of microbial activity, microbial growth, substrate acetate limitation, and the existence of anoxic microenvironments within soil particles. The predicted fluxes generally exceed our field observations and describe an envelope that contains nearly all of our measurements (Figure 6). Based on this comparison, we estimate that approximately half of the methane produced in the uppermost 30 cm of soil is oxidized in situ, consistent with the detection of methanotrophy throughout the soil column. Unfortunately, a quantitative comparison between total oxidation rates and rate constants requires unavailable information about the rate of CH_4 transport (often in bubbles) through soil and soil pore space. A methane-consumption efficiency of 50% is within the range of values in the literature (30–90%)

(van der Nat and Middelburg 1998, Ding et al. 2004).

The emergent macrophyte *Schoenoplectus lacustris*, for which we have tentative evidence for methane oxidation, has an aerenchymous system and has previously been identified as a conduit of methane from a lake (Kankaala et al. 2003). It is a plausible host for a methane-oxidizing microbial community. However, the lack of consistent activity from sample to sample or plant to plant suggests that such a community is not widely present or active in this wetland and that methane oxidation is primarily restricted to the soil.

Our data constitute indirect evidence for the dynamics of the methanogenic and methanotrophic communities in Ka'au Crater. The high potential methane production in the 28 March core from the honohono vegetation pattern (Figure 3) could have been a consequence of high precipitation and persistently elevated water-table levels during the previous 25 days (Figure 2). The other profiles, all exhibiting lower potential methane production, were obtained during a relatively drier period when the water-table level was falling (Figure 2). Conversely, the high rate constants of methane oxidation observed in the 5 May core from the 'ōhi'a pattern could be a consequence of falling water-table levels that have allowed methanotrophs to flourish (Figure 2).

Although we find no significant correlation between profile-integrated potential methane generation and CH_4 oxidation rate constants, we point out that *rates* of CH_4 oxidation should nonetheless vary with methane production due to first-order kinetics. This raises the possibility that increased methane oxidation by methanotrophs may partly compensate for variation in methane production by changes in water-table level. The population dynamics of both methanogens and methanotrophs subject to rapid water-table fluctuations may also obscure any correspondence between that water-table level and net methane emission. Another contributing factor may be the inability of strictly anaerobic methanogens to flourish in the upper 15 cm of soil where the water-table level and oxygen concentrations fluctuate greatly. Further studies in wetland systems with a dynamic and predictable hydrology such as the Ka'au Crater bog could test these hypotheses.

ACKNOWLEDGMENTS

We thank Aly El-Kadi and Robert Whittier for the use of water-level sensors and Fred Mackenzie, Jane Schoonmaker, and Frank Sansone for advice. Access to Ka'au Crater was by permit obtained from the Honolulu Board of Water Supply. We also thank two anonymous reviewers for their useful suggestions on the manuscript.

Literature Cited

Bartlett, D. S., K. B. Bartlett, J. M. Hartman, R. C. Harriss, D. I. Sebacher, R. Pelletier-Travis, D. D. Dow, and D. P. Brannon. 1989. Methane emissions from the Florida Everglades: Patterns of variability in a regional wetland ecosystem. Glob. Biogeochem. Cycles 3:363–374.

Bartlett, K. B., P. M. Crill, J. A. Bonassi, J. E. Richey, and R. C. Harriss. 1990. Methane flux from the Amazon River floodplain: Emissions during rising water. J. Geophys. Res. 95:16,773–16,788.

Bartlett, K. B., and R. C. Harriss. 1993. Review and assessment of methane emissions from wetlands. Chemosphere 26:261–320.

Chapin, F. S., A. D. McGuire, J. Randerson, R. Pielke, D. Baldocchi, S. E. Hobbie, N. Roulet, W. Eugster, E. Kasischke, E. B. Rastetter, S. A. Zimov, and S. W. Running. 2000. Arctic and boreal ecosystems of western North America as components of the climate system. Glob. Change Biol. 6:211–223.

Devol, A. H., J. E. Richey, B. R. Forsberg, and L. A. Martinelli. 1990. Seasonal dynamics in methane emissions from the Amazon River floodplain to the troposphere. J. Geophys. Res. 95:16,417–16,426.

Ding, W., Z. Cai, and D. Wang. 2004. Preliminary budget of methane emissions from natural wetlands in China. Atmos. Environ. 38:751–759.

Dlugokencky, E. J., K. A. Masarie, P. M. Lang, and P. P. Tans. 1998. Continuing decline in the growth rate of the atmo-

spheric methane burden. Nature (Lond.) 393:447–450.
Elliot, M. E., and E. M. Hall. 1977. Wetlands and wetland vegetation of Hawaii. U.S. Army Corps of Engineers, Pacific Ocean Division, Honolulu, Hawai‘i.
Funk, D. W., E. P. Pullman, K. M. Peterson, P. M. Crill, and W. D. Billings. 1994. Influence of water table on carbon dioxide, carbon monoxide, and methane fluxes from taiga bog microcosms. Glob. Biogeochem. Cycles 8:271–278.
Gerard, G., and J. Chanton. 1993. Quantification of methane oxidation in the rhizosphere of emergent aquatic macrophytes: Defining upper limits. Biogeochemistry 23:79–97.
Harriss, R. C., D. I. Sebacher, K. B. Bartlett, D. S. Bartlett, and P. M. Crill. 1988. Sources of atmospheric methane in the South Florida environment. Glob. Biogeochem. Cycles 2:231–243.
Heilman, M. A., and G. Carlton. 2001. Methane oxidation associated with submerged vascular macrophytes and its impact on plant diffusive methane flux. Biogeochemistry 52:207–224.
Hotchkiss, S., and J. O. Juvik. 1999. A late-Quaternary pollen record from Ka‘au Crater, O‘ahu, Hawai‘i. Quat. Res. 52:115–128.
Intergovernmental Panel on Climate Change. 2001. Climate change 2001: The scientific basis. IPCC, Cambridge.
Kankaala, P. S., I. Makela, E. Bergstrom, T. Huitu, A. Kaki, M. Ojala, P. Rantakari, G. Kortelainen, and L. Arvola. 2003. Midsummer spatial variation in methane efflux from stands of littoral vegetation in a boreal meso-eutrophic lake. Freshwater Biol. 48:1617–1629.
Kennedy, E. 1975. Ka‘au Crater: A study of plant patterns in a Hawaiian bog. M.A. thesis, University of Hawai‘i at Mānoa, Honolulu.
Kettunen, A., V. Kaitala, J. Alm, J. Silvola, H. Nykänen, and P. J. Martikainen. 2000. Predicting variations in methane emissions from boreal peatlands through regression models. Boreal Environ. Res. 5:115–131.
Khalil, M. A. K., R. A. Rasmussen, and M. J. Shearer. 1998. Flux measurement and sampling strategies: Applications to methane emissions from rice fields. J. Geophys. Res. 103:25,211–25,218.
Knapp, A. K., and J. B. Yavitt. 1992. Evaluation of closed-chamber method for estimating methane emissions from aquatic plants. Tellus Ser. B Chem. Phys. Meteorol. 44:63–71.
Le Mer, J., and P. Roger. 2001. Production, oxidation, emission and consumption of methane by soils: A review. Eur. J. Soil Biol. 37:25–50.
Macdonald, G. A., A. A. Abbott, and F. L. Peterson. 1983. Volcanoes in the sea: The geology of Hawaii. 2nd ed. University of Hawai‘i Press, Honolulu.
Marani, L., and P. C. Alvala. 2007. Methane emissions from lakes and floodplains in Pantanal, Brazil. Atmos. Environ. 41:1627–1633.
Milich, L. 1999. The role of methane in global warming: Where might mitigation strategies be focused? Glob. Environ. Change 9:179–201.
Moore, P. D. 2002. The future of cool temperate bogs. Environ. Conserv. 29:3–20.
Moore, T. R., A. Heyes, and N. T. Roulet. 1994. Methane emissions from wetlands, southern Hudson Bay lowland. J. Geophys. Res. 99:1455–1468.
Oki, D. S., S. B. Gingerich, and R. L. Whitehead. 1999. Ground water atlas of the United States: Alaska, Hawaii, Puerto Rico and the U.S. Virgin Islands. U.S. Geological Survey.
Pino, J. A., A. Bello, A. Urquiola, R. Marbot, and M. P. Marti. 2004. Leaf oils of *Psidium parvifoium* Griseb and *Psidium cattleianum* Sabine from Cuba. J. Essent. Oil Res. 16:370–371.
Rask, H., J. Schoenau, and D. Anderson. 2002. Factors influencing methane flux from a boreal forest wetland in Saskatchewan, Canada. Soil Biol. Biochem. 34:435–443.
Roslev, P., and G. M. King. 1996. Regulation of methane oxidation in a freshwater wetland by water table changes and anoxia. FEMS Microbiol. Ecol. 19:105–115.
Schütz, H., and W. Seiler. 1989. Methane

flux measurements: Methods and results. Pages 209–228 *in* M. O. Andrae and D. S. Schimmel, eds. Exchange of trace gases between terrestrial ecosystems and the atmosphere. John Wiley & Sons, New York.

Segers, R. 1998. Methane production and methane consumption: A review of processes underlying wetland methane fluxes. Biogeochemistry 41:23–51.

Van der Nat, W. A., and J. J. Middelburg. 1998. Seasonal variation in methane oxidation by the rhizosphere of *Phragmites australis* and *Scirpus lacustris*. Aquat. Bot. 61:95–110.

Van Hulzen, J. B., R. Segers, P. M. Van Bodegom, and P. A. Leffelaar. 1999. Temperature effects on soil methane production: An explanation for observed variability. Soil Biol. Biochem. 31:1919–1929.

Van Lierop, W. 1990. Soil pH and lime requirement determination. Pages 73–126 *in* R. L. Westerman, ed. Soil testing and plant analysis. Soil Science Society of America, Madison, Wisconsin.

Watterson, I. G., and M. R. Dix. 2003. Simulated changes due to global warming in daily precipitation means and extremes and their interpretation using the gamma distribution. J. Geophys. Res. 108:4379.

Wetherald, R. T., and S. Manabe. 2002. Simulation of hydrologic changes associated with global warming. J. Geophys. Res. 107:4379.

Wuebbles, D. J., and K. Hayhoe. 2002. Atmospheric methane and global change. Earth Sci. Rev. 57:177–210.

Appendix 1

Net Methane-Emission Measurements

	Date (ddmmyy)	Loc.[a]	Δt (min)	N	C_0 (ppm)	Cf (ppm)	Flux (mg m^{-2} day^{-1})	χ^2_υ	Notes[b]
1	30/08/03	G	120	5	1.8	2	N/D	0.02	Nondetection
2	7/9/03	H	120	5	3.7	15.3	76.9	0.36	S
3	21/09/03	H	120	5	3	13.3	69.2	0.42	S
4	21/09/03	S	120	5	2.2	3.5	9	0.04	
5	29/09/03	H	120	5	3	14.7	71.1	1.38	S
6	29/09/03	O	90	5	16	36.6	215.2	0.91	Flux excluded
7	5/10/03	H	120	5	2.4	10.9	56.6	0.72	S
8	5/10/03	O	60	5	12.9	36.9	223.2	19.12	Flux excluded
9	12/10/03	H	120	6	3.1	11	54.9	0.47	S
10	12/10/03	S	120	6	3.8	7.6	25.5	0.24	15 min pt. excluded
11	18/10/03	H	120	6	2.8	16.4	87	0.4	S
12	18/10/03	H	120	6	3.9	15.7	80.7	0.38	S
13	18/10/03	H	120	6	2	13.8	76.9	0.56	S
14	18/10/03	H	120	6	3.8	19.5	93.5	0.45	S
15	25/10/03	H	105	6	3.2	25	96.1	0.66	0 min pt. excluded, S
16	25/10/03	G	120	6	2.2	4	11.4	0.07	
17	2/11/03	H	120	6	3.1	17.3	91.9	0.21	S
18	2/11/03	S	120	6	2.4	5.1	16.8	0.03	90 min pt. excluded
19	11/2/04	H	90	5	7.4	27.3	171.7	0.12	V, S
20	11/2/04	H	90	5	4.4	26.4	189.5	0.27	V, S
21	11/2/04	H	90	5	4.5	21	145	0.34	30 min pt. excluded, V, S
22	11/2/04	H	90	5	3	19.4	145.6	0.54	V, S
23	18/02/04	H	90	5	4.9	35	305.6	4.42	90 min pt. excluded, V, S
24	18/02/04	H	90	5	4.8	40.9	337.5	2.7	90 min pt. excluded, V, S
25	18/02/04	H	90	5	4.1	23.2	166.1	0.49	V, S
26	18/02/04	H	90	5	3.5	23.3	174.7	0.28	V, S
27	25/02/04	H	90	5	3.2	19	135.5	1.9	V, S
28	25/02/04	H	90	5	5	23	146.8	1.79	V, S

Appendix (continued)

	Date (ddmmyy)	Loc.[a]	Δt (min)	N	C_0 (ppm)	Cf (ppm)	Flux (mg m^{-2} day^{-1})	χ^2_v	Notes[b]
29	25/02/04	H	90	5	3	17.2	123.5	0.99	V, S
30	25/02/04	H	90	5	3.5	19.4	136.5	1.36	V, S
31	9/3/04	H	90	5	17.6	36.8	162.9	2.14	Flux excluded
32	9/3/04	H	90	5	3.6	21.2	156.2	0.25	S
33	9/3/04	H	90	5	13.8	25.4	102	0.08	V, S
34	9/3/04	H	90	5	4.7	17.1	109.3	0.07	V, S
35	17/03/04	H	90	5	6	29.1	200.3	0.69	V, S
36	17/03/04	H	90	5	2.8	26.9	209.4	0.18	V, S
37	17/03/04	H	90	5	6.7	23.7	145	1.21	V, S
38	17/03/04	H	90	5	3.1	21.2	155.5	0.16	V, S
39	28/03/04	H	90	4	3.2	23.6	175	0.39	V, S
40	28/03/04	H	90	4	4.2	23.9	170.6	0.83	V, S
41	28/03/04	H	60	4	7.2	25.4	89.7	0.28	0 min pt. excluded, V, S
42	28/03/04	H	90	4	4.7	15.5	94.1	0.04	V, S
43	31/03/04	H	90	4	4.8	19.5	125.4	0.68	V, S
44	31/03/04	H	90	4	2.8	17.4	126.7	0.09	V, S
45	31/03/04	H	90	4	4.5	17.1	108.4	1	V, S
46	31/03/04	H	90	4	4.6	15.7	96.3	0.06	V, S
47	6/4/04	H	90	4	7.7	40.4	289.2	3.2	90 min pt. excluded, V, S
48	6/4/04	H	90	4	4.6	35.7	318.2	0.07	90 min pt. excluded, V, S
49	6/4/04	H	90	4	9.7	29.8	174.3	0.16	V, S
50	6/4/04	H	90	4	8.1	29.4	187	0.17	30 min pt. excluded, V, S
51	13/04/04	H	90	4	14.8	35.7	179.3	5.45	Flux excluded
52	13/04/04	H	90	4	2.5	21.4	163.6	0.09	S
53	13/04/04	G	60	4	9.8	35.9	115.4	18.42	Flux excluded
54	13/04/04	G	90	4	7.2	16.7	86.5	3.03	30 min pt. excluded
55	21/04/04	H	90	4	10.1	35.5	254.7	0.07	90 min pt. excluded, S
56	21/04/04	H	90	4	2.5	27.8	219.5	0.36	S
57	21/04/04	G	90	4	20.8	23	19	2.37	
58	21/04/04	G	90	4	6.5	6.8	N.D	0.24	Nondetection
59	28/04/04	H	90	4	13.4	48.8	313.2	4.39	Flux excluded
60	28/04/04	H	90	4	6.2	39	283.6	9.93	Flux excluded
61	28/04/04	G	90	4	2.9	7.6	25.8	0.23	
62	28/04/04	G	90	4	3.3	5.1	15.1	0.22	
63	5/5/04	H	90	4	15.7	30.2	196.7	1.06	90 min pt. excluded, S
64	5/5/04	H	90	4	6.8	24.4	172.9	1.27	S
65	5/5/04	O	60	4	24.8	29.8	234.4	0.4	90 min pt. excluded
66	5/5/04	O	90	4	9.7	11.5	57.9	8.82	Flux excluded
67	11/5/04	H	90	4	15.7	51	312.2	10.91	Flux excluded
68	11/5/04	H	90	4	6.8	38.8	295.6	1.34	90 min pt. excluded, S
69	11/5/04	O	90	4	24.8	39.3	132.7	2.69	Flux excluded
70	11/5/04	O	90	4	9.7	18	77.7	1.2	
71	20/05/04	H	60	4	19.8	66.7	592.3	40.1	Flux excluded
72	20/05/04	H	60	4	10.8	56.1	455.8	3.91	Flux excluded
73	20/05/04	G	480	7	5.1	16.6	15.1	7.02	
74	25/05/04	H	90	4	13.1	42.5	258.6	18.05	Flux excluded
75	25/05/04	H	90	4	7.5	35.5	280.1	0.11	90 min pt. excluded, S
76	25/05/04	O	60	4	18.5	26.8	6.9	0.62	0 min pt. excluded
77	25/05/04	O	90	4	3.2	4	8.1	0.05	
78	13/06/04	H	120	61	71.1	87.7	161.7	47.84	Flux excluded
79	21/06/04	H	60	10	2.7	12	110.6	0.34	New location, S
80	21/06/04	H	60	10	3.5	13.8	126.2	0.23	Replicate sampling, S
81	12/8/04	H	30	4	2		49.8	0.06	Replicate sampling, S
82	12/8/04	H	30	4	1.9		64.2	0.01	Replicate sampling, S

[a] G, strawberry guava; H, honohono; O, ʻōhiʻa; S, sedge.
[b] V, variability data; S, seasonal data.